Thickness Measurement of a Metal Sheet by an Adaptive Two-Wave Mixing Interferometer

Duan Changqi Chen Jian He Sailing

Centre for Optical and Electromagnetic Research, Zhejiang Provincial Key Laboratory for Sensing Technologies, State Key Laboratory of Modern Optical Instrumentation, Zhejiang University, Hangzhou, Zhejiang 310058, *China*

Abstract Measuring the thickness of metal sheets is an issue of great importance in production facilities and in other industrial applications. The conventional triangulation method is not suitable for the detection of rough surfaces and semitransparent or multi-scattering materials. Therefore, an adaptive two-wave mixing interferometer based on the photorefractive $Bi_{12}SiO_{20}$ (BSO) crystal is designed to measure the thickness of an aluminum metal sheet. A holographic grating, formed by the photorefractive effect, diffracts both the signal beam and the reference beam to demodulate the ultrasonic vibration. The system, in which the low frequency noise caused by the environmental perturbation can be filtered automatically through the dynamic holography grating, is demonstrated to be a highly sensitive, convenient, and inexpensive non-contact technique for thickness measurement and ultrasonic vibration detection on rough surfaces. The technique has the potential for the detection of hidden defects, especially when it is combined with laser ultrasonic technology.

Key words measurement; two-wave mixing; holography grating; metal sheet; ultrasonic

OCIS codes 120.3180; 050.1950

基于自适应双波混合干涉仪的金属板厚度测量

段昌琪 陈 剑* 何赛灵

浙江大学现代光学仪器国家重点实验室, 浙江省传感重点实验室, 光及电磁波研究中心, 浙江 杭州 310058

摘要 在钢板的生产和使用过程中,钢板厚度的测量极其重要。传统的激光三角法不适合测量粗糙表面物体和多散射介质的厚度。基于硅酸铋光折变晶体搭建了一套自适应的双波混合干涉仪系统,使用该系统精确测量了铝块的厚度。由于光折变效应形成的全息光栅使信号光和参考光发生衍射,解调出超声振动信号。动态全息光栅的形成,能自动滤除环境引起的低频扰动。该系统在厚度测量、粗糙面超声振动测量中具有灵敏度高、调节方便、非接触、价格相对便宜等特点,将来与激光超声技术相结合在内部缺陷检测上有非常广阔的前景。

关键词 测量; 双波混合; 全息光栅; 金属板; 超声

中图分类号 TH741; O438.1 **文献标识码** A

doi: 10.3788/CJL201542.0808002

1 Introduction

Accurately measuring the dimensions of metal sheets by automated, non-contact methods become an increasingly important issue. The thickness must be monitored during metal production to improve quality and yield; measurements are also required during practical applications to ensure good performance[1]. To meet these needs, several non-contact optical methods have been used to detect the thickness of metal sheets, such as double-sided laser point triangulation[1-2], light attenuation, and autofocus[3] techniques. The best-known technique, which is

收稿日期: 2015-03-02; **收到修改稿日期**: 2015-04-17

基金项目: 国家自然科学基金(61401392)、中国博士后科学基金(2014M551729)

作者简介: 段昌琪(1991—),男,硕士研究生,主要从事光学精密测量方面的研究。E-mail: duanchangqi@zju.edu.cn

导师简介: 何赛灵(1966—),男,教授,博士生导师,主要从事生物光学、光学测量等方面的研究。E-mail: sailing@jorcep.org

*通信联系人。E-mail: mechenjian@zju.edu.cn

widely used in industry, is the cheap, reliable, and accurate triangulation method. However, this method is not useful in the case of rough surfaces, or for semitransparent or multi-scattering materials[2].

One of the most effective methods for vibration measurement[4-6] is the optical interferometer[7]. However, the sensitivity of this technique in non-laboratory conditions is restricted, as the signal and the reference wave front interfering at the photodetector must be adjusted to keep their average phase shift constant[8]. A two-wave mixing[9] interferometer (TWMI) can solve both problems when the conventional beam splitter is replaced by a dynamic hologram continually recorded in a photorefractive crystal (PRC). This technique is also called adaptive interferometry[10]. The highest sensitivity to small phase modulation can be achieved when the PRC is under a strong direct current field[11]. The TWMI can be used to detect the vibration of rough surfaces[12-14], eliminating all unwanted low-frequency noise generated by the environment[15-16].

In this study, a TWMI was designed to detect ultrasonic vibrations on a metal surface, and the thickness of an aluminum (Al) block was measured. The experimental result agree closely with ultrasonic probe measurements and with the thickness determined by a vernier caliper.

2　Photorefractive Effect and Two-Wave Mixing in a Crystal

The photorefractive effect, in which the refractive index of a crystal changes because of the spatial distribution of illumination intensity, is a nonlinear optical phenomenon. When two coherent laser beams interfere with each other in the $Bi_{12}SiO_{20}$ (BSO) crystal, a spatial distribution of light intensity will be formed, and an index grating is built up through the photorefractive effect, as shown in Fig.1.

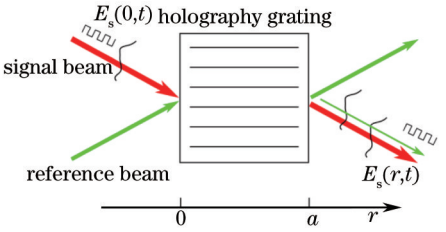

Fig.1　Schematic diagram of two-wave mixing mechanism

The two beams, called the signal beam and the reference beam, are diffracted by the newly formed grating. The diffracted light of the reference beam is in the same direction with the transmitted signal beam and their phase structures are also the same. When the phase modulation of the signal beam is much faster than the response time of the photorefractive effect, the grating can be regarded as stationary.The amplitude of the transmitted signal beam in the undepleted pump approximation can be expressed[17] as

$$E_s(r,t)=\exp\left(-\frac{\alpha r}{2}\right)E_s(0,0)\{[\exp(\gamma r)-1]+\exp[\mathrm{i}\varphi(t)]\}\,, \tag{1}$$

and the incident signal beam amplitude is

$$E_s(0,t)=E_s(0,0)\exp[\mathrm{i}\varphi(t)]\,, \tag{2}$$

where α is the absorption coefficient of the crystal, γ is the photorefractive amplitude gain[17-18], and r is the thickness of the crystal. Generally, γ is a complex quantity, the modulus of which is associated with the strength of the grating while the phase represents the spatial phase difference of the index grating and the light intensity distribution. In Eq.(1), the term $[\exp(\gamma r)-1]$ represents the diffracted reference beam and the term $\exp[\mathrm{i}\varphi(t)]$ is the transmitted signal beam.

If the phase modulation is relatively small, that is, $\varphi(t)\ll\pi/2$, the intensity of the output signal beam can be calculated as

$$I_s(r,t)=\exp(-\alpha r)I_s(0,0)[\exp(2\gamma' r)+2\exp(\gamma' r)\sin(\gamma'' r)\varphi(t)]\,, \tag{3}$$

where $\gamma=\gamma'+\mathrm{i}\gamma''$. In the diffusion regime, γ'' is equal to zero, which means that the sensitivity to the small phase

modulation is nearly zero. The maximum sensitivity is obtained when the two beams are in quadrature. In the drift regime, possibly under an external electric field, the phase between the two incident light beams is almost in quadrature.

3　Experimental Setup

3.1 Optical Path Design

The TWMI based on BSO is depicted in Fig.2. The small diameter 532 nm laser beam, which is emitted from a Cobolt laser whose maximum output power is 1 W, is expanded to the desired size by the beam expander. It is then divided into two parts—a reference beam and a signal beam—by the polarized beam splitter (PBS). The half wave plate before the PBS is used to adjust the ratio of the two beams. One of the advantages of the two-wave-mixing interferometer is its ability to measure the vibration of a rough surface. The scattered light is collected from the rough surface and its polarization is rotated by a quarter wave plate to be the same as that of the reference beam. The two beams interfere with each other in the BSO crystal. Due to the photorefractive effect and the two-wave mixing in the BSO, the small phase modulation can be measured by the detector in the direction of the signal beam.

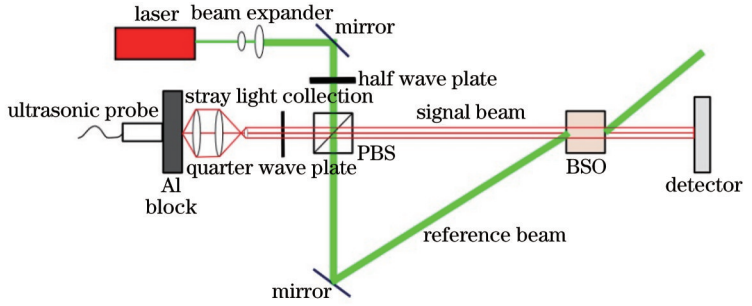

Fig.2 Schematic diagram of TWMI

3.2 Photorefractive BSO under External Direct Current Field

BSO is a cubic crystal with good photorefractive properties[19-21]. The BSO used is cut in the [001], [110] and [1 $\bar{1}$ 0] directions with a size of 5 mm×5 mm×5 mm. A high voltage near 3.5 kV was applied along the [001] direction, making the BSO work in the drift regime. In addition, the voltage can also increase the coupling constant to obtain a high sensitivity. The BSO is placed as shown in Fig.3(a).

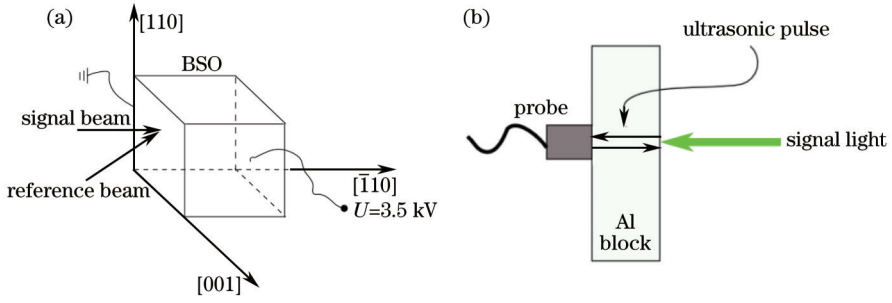

Fig.3 (a) Placement of BSO crystal and direction of external electric field; (b) Al block test sample

3.3 Sample Testing

The TWMI designed above is used to measure the thickness of an Al block. A longitudinal wave ultrasonic probe, matched with an ultrasonic fault detector, is placed behind the Al block [Fig.3(b)]. The probe excites ultrasonic pulses with a frequency of 1 kHz. Each pulse travels back and forth due to the interface reflection, and decays gradually. These pulses are detected by the TWMI at the front surface and by the probe at the rear surface.

4　Experimental Result and Analysis

Fig.4(a) shows the detected signal by the TWMI. The raw signal is mixed with noise, whose low frequency part mainly comes from the fluctuation of the output power of the laser. Therefore, the signal is filtered by Matlab, with the result

shown in Fig.4(b). The time interval between two pulses, which equals the time that the ultrasonic pulse travels in the Al block for a single cycle, is determined by the thickness of the sample. As expected, the time between every two adjacent pulses is equal. The amplitude of the pulse decays due to the energy loss of the ultrasonic pulse.

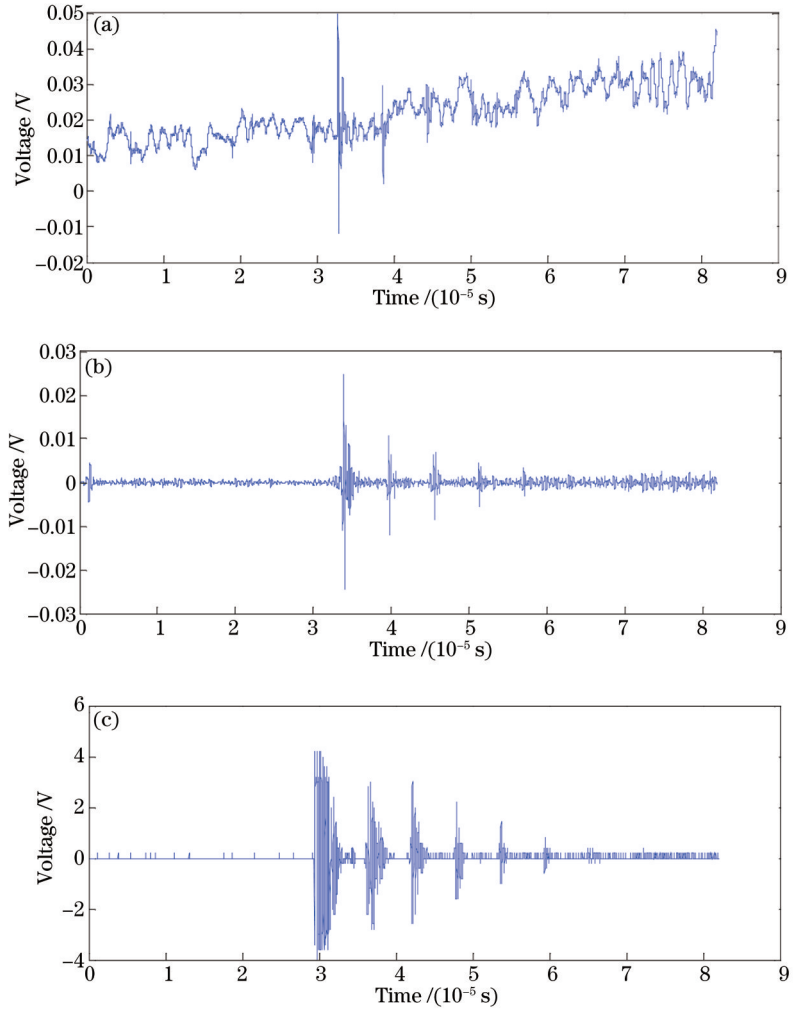

Fig.4 (a) Signal detected by TWMI; (b) signal after filtering; (c) signal detected by the ultrasonic probe

The thickness can be expressed as

$$D = \Delta t \cdot v/2 \,, \tag{4}$$

where D represents the thickness, Δt represents the time between two adjacent pulses, and v represents the velocity of the ultrasonic pulse in the Al block. As shown in Fig.4(b), the time interval of the first four pulses is selected to calculate the Δt:

$$\Delta t = \frac{1.7312 \times 10^{-5}}{3}\text{s} = 5.7707 \times 10^{-6}\text{s} \,. \tag{5}$$

Generally, v=6300 m/s, so the thickness D is 1.8178 cm. Experimental results obtained by the TWMI method, the ultrasonic probe, and a vernier caliper are compared in Table 1.

Table 1 Thickness measurement results by three methods

Data source	Thickness /cm	Relative error /%
By TWMI	1.8178	0.67
By ultrasonic probe	1.8136	0.90
By vernier caliper	1.830	0

The thickness measured by the vernier caliper is regarded as the true value and the relative errors are calculated on that basis. An extremely low relative error and high precision are confirmed. On the other hand, the difference in

the thicknesses measured by TWMI and by the ultrasonic probe is quite small, while both are somewhat large compared to the result measured by the vernier caliper. This is mainly due to the inaccuracy of the ultrasonic velocity in the aluminum. The relative error between the value measured by TWMI and by the ultrasonic probe is only 0.23% and the thickness difference is only 42 μm. Thus, the excellent agreement between the two methods, and the high accuracy of the TWMI method are demonstrated.

5 Conclusion

A TWMI based on photorefractive BSO under high voltage is used to measure the thickness of a metal block. A comparison of the results measured by three methods is made to demonstrate the high precision of the TWMI method. The TWMI method has the following advantages: high sensitivity, no need for a severe optical path, automatic elimination of low frequency fluctuations and suitability for rough surface detection. Moreover, the method shows promise for the future when combined with laser ultrasonic technology in non-contact nondestructive measurement situations; it is suitable for high temperature conditions and other harsh environments.

References

1 P Lehtonen, J Miettinen, H Keränen, *et al*.. Metal sheet thickness profile measurement method based on two-side line triangulation and continuous vibration compensation[C]. SPIE, 2008, 2008, 7003: 70030P.

2 A Nadeau, L Pouliot, F Nadeau, *et al*.. A new approach to online thickness measurements of thermal spray coatings[J]. J Thermal Spray Technology, 2006, 15(4): 744-749.

3 K C Fan, C L Chu, J I Mou. Development of a low-cost autofocusing probe for profile measurement[J]. Meas Sci & Technol, 2001, 12 (12): 2137-2146.

4 Guo Yongxing, Zhang Dongsheng, Zhou Zhude, *et al*.. Research progress in fiber-Bragg-grating accelerometer[J]. Laser & Optoelectronics Progress, 2013, 50(6): 060001.
郭永兴, 张东生, 周祖德, 等. 光纤布拉格光栅加速度传感器研究进展[J]. 激光与光电子学进展, 2013, 50(6): 060001.

5 Tang Weijie, Fu Lei, Chen Shufen, *et al*.. Realization of measuring micro-vibration based on phase generated carrier modulation-demodulation method and interference analysis[J]. Chinese J Lasers, 2013, 40(2): 0214001.
唐伟杰, 付　雷, 陈淑芬, 等. 相位生成载波调制解调法测量微振动的实现及干扰分析[J]. 中国激光, 2013, 40(2): 0214001.

6 Lu Wengao, Sun Qizhen, Wo Jianghai, *et al*.. High sensitivity micro-vibration sensor based on distributed Bragg reflector fiber laser[J]. Acta Optica Sinica, 2014, 34(7): 0728006.
鲁文高, 孙琪真, 沃江海, 等. 基于分布布拉格反射光纤激光器的高灵敏度微振动传感器[J]. 光学学报, 2014, 34(7): 0728006.

7 P Hariharan. Optical interferometry[C]. Reports on Progress in Physics, 1991, 54 (3): 339-390.

8 A A Kamshilin, R V Romashko, Y N Kulchin. Adaptive interferometry with photorefractive crystals[J]. J Appl Phys, 2009, 105(3): 031101.

9 J P Huignard, A Marrakchi. Two-wave mixing and energy transfer in $Bi_{12}SiO_{20}$ crystals: application to image amplification and vibration analysis[J]. Opt Lett, 1981, 6(12): 622-624.

10 T J Hall, M S Ner, M A Fiddy. Detector for an optical-fiber acoustic sensor using dynamic holographic interferometry[J]. Opt Lett, 1980, 5(11): 485-487.

11 L Young, W K Y Wong, M L W Thewalt, *et al*.. Theory of formation of phase holograms in lithium niobate[J]. Appl Phys Lett, 1974, 24(6): 264-265.

12 A Blouin, J P Monchalin. Detection of ultrasonic motion of a scattering surface by two-wave mixing in a photorefractive GaAs crystal[J]. Appl Phys Lett, 1994, 65(8): 932-934.

13 D M Pepper, P V Mitchell, G J Dunning, *et al*.. Double-pumped conjugators and photo-induced EMF sensors: two novel, highbandwidth, auto-compensating, laser-based ultrasound nondestructive characterization of materials detectors[C]. Materials Science Forum, 1996, 210: 425-432.

14 P Delaye, A Blouin, D Drolet, *et al*.. Detection of ultrasonic motion of a scattering surface by photorefractive InP: Fe under an applied dc field[J]. J Opt Soc Am B, 1997, 14(7): 1723-1734.

15 Y Qiao, Y Zhou, S Krishnaswamy. Adaptive demodulation of dynamic signals from fiber Bragg gratings using two-wave mixing

technology[J]. Appl Opt, 2006, 45(21): 5132-5142.

16 R V Romashko, Y N Kulchin, S M Shandarov, *et al*.. Adaptive correlation filter based on dynamic reflection hologram formed in photorefractive $Bi_{12}TiO_{20}$ crystal[J]. Opt Rev, 2005, 12(1): 58-60.

17 P Delaye, L A De Montmorillon, G Roosen. Transmission of time modulated optical signals through an absorbing photorefractive crystal[J]. Opt Commun, 1995, 118(1): 154-164.

18 N V Kukhtarev, V B Markov, S G Odulov, *et al*.. Holographic storage in electrooptic crystals. II beam coupling-light amplification[J]. Ferroelectrics, 1979, 22(14): 961-964.

19 L F Magana, I Casar, J G Murillo. Beam energy exchange in sillenite crystals ($Bi_{12}SiO_{20}$ and $Bi_{12}TiO_{20}$), considering the variation of light modulation along sample thickness in a strong non-linear regime[J]. Opt Mater, 2008, 30(6): 979-986.

20 R A Ganeev, A I Ryasnyansky, R I Tugushev, *et al*.. Nonlinear optical characteristics of BSO and BGO photorefractive crystals in visible and infrared ranges[J]. Opt Quantum Electron, 2004, 36(9): 807-818.

21 R V Romashko, A I Grachev, Y N Kulchin, *et al*.. Fast photogalvanic response of a $Bi_{12}SiO_{20}$ crystal[J]. Opt Express, 2010, 18(26): 27142-27154.

栏目编辑：何卓铭